Solid State Phenomena
ISSN: 1662-9779, Vol. 388, pp 187-197
doi:10.4028/p-6D4Y1c

Submitted: 2026-01-19
Revised: 2026-02-24
Accepted: 2026-02-24
Online: 2026-04-15

The Influence of Uphill Quench on the Microstructure and Properties of Particle-Reinforced Aluminum Matrix Composites

Ran Pan[1,2,3,a*], Baosheng Liu[1,2,3,b], Nan Guo[4,c], Yuansong Zeng[1,2,3,d], Yunhe Chang[1,2,3,e], Zhiyong Li[4,f]

[1]AVIC Manufacturing Technology Institute, Beijing 100024, China

[2]China Aeronautical Key Laboratory for Plastic Forming Technologies, Beijing, 100024, China

[3]Beijing Key Laboratory of Digital Plastic Forming Technology and Equipment, Beijing, 100024, China

[4]AVIC Changhe Aircraft Industry (Group) Corporation LTD., Jingdezhen, China

[a*]bkdpanran@163.com,[b]herr.liubaosheng@163.com, [c]116049213@qq.com, [d]yszeng@hotmail.com, [e]cyh186010456852000@163.com, [f]dandingchi2022@qq.com

Keywords: particle-reinforced aluminum composite, residual stress, uphill quench.

Abstract. Various heat treatments were applied to reduce quench-induced residual stresses while improving the mechanical properties of particle-reinforced aluminum composite. The residual stress distribution of samples quenched in water with different cooling media was measured. The results showed that quenching with the 30% polyethylene glycol quenchant (PAG) yields up to an 86.8% reduction in residual stress magnitude compared with cold-water quenching (CWQ). Still, the tensile properties of samples quenched in 30% polyethylene glycol quenchant were low, with a 12.5% reduction in yield strength. The experimental results show that the uphill quench (UQ) method is an effective means of reducing residual stresses induced by quenching. At the same time, the effect on tensile properties is negligible. Moreover, the study found that combining uphill quenching with short-aging treatment can further improve the residual stress, strength, and fracture toughness of SiCp/Al-Cu-Mg composites.

Introduction

As compensation for the lower ductility compared to unreinforced aluminum alloys, particulate-reinforced aluminum matrix composites (AMCs) exhibit significantly improved specific modulus, making them competitive in the aerospace and automotive industries [1, 2]. One key to achieving good mechanical properties of AMCs lies in the formation of a supersaturated solid solution. This microstructure of aluminum alloys/composites can only be obtained by quenching the material from the solution treatment temperature to make most solute elements' freeze' in a solid solution. However, during rapid cooling, high-amplitude residual stresses (approaching the yield stress of the quenched material) are generated due to the large temperature gradient between the core and surface of large-sized materials (thickness > 50 mm) and the non-uniform plastic deformation caused by thermal strain. These internal stresses can lead to unacceptable deformation or cracking in subsequent processing after quenching, severely affecting fatigue crack propagation behavior and material service life [3, 4].

Uphill quenching, although termed a ‘cryogenic’ process, should not be mistaken for merely exposing parts to a cryogenic environment. Its mechanism is that during the process of rapidly heating the ultra-low temperature material to the temperature of a high-temp medium, the newly thermal stress caused by the large internal and external temperature difference in the material is superimposed on the quench-induced residual stress, which causes the material to yield, thereby releasing the original residual stress. In contrast to quite limited data about the uphill quench effect on residual stresses in aluminum composites, for heat-treatable aluminum alloys, many research results have shown that the uphill quench process is an effective and highly efficient method that can relieve the quench-induced residual stresses in the material, ranging from 20%~80%[5-7]. The technique can be adapted to critical components with complex geometries, e.g., forgings.

Given the crucial role of aluminum matrix composites in the aerospace industry, this study aims to investigate the effects of quenching processes using 30% PAG solution or water as the cooling medium, uphill quenching, and uphill quenching combined with aging treatment on the residual stress and microstructure of heat-treated particle-reinforced aluminum matrix composites. Furthermore, the study examines the effects of these heat-treatment methods on the mechanical properties of heat-treated aluminum matrix composites.

Experiment

Experimental Design

15%vol SiCp/Al-Cu-Mg composite has been used in this work. In this study, the actual composition of the Al-Cu-Mg matrix was Al-3.51Cu-1.35Mg-Fe0.06-Si0.29 (wt. %). The average size of SiC particles in the composite was 7μm. The composite was manufactured using powder metallurgy (PM) technology, followed by hot extrusion at 480℃ and then forging to a Ø250 mm × 100 mm. The block specimens for various heat treatments were machined by wire-ESR cutting from 15%vol SiCp/Al-Cu-Mg composite forgings. This study used 80mm × 85mm × 85mm aluminum matrix composite blocks, with the thickness direction (80mm) aligned with the forging direction. The micrograph of one particle-reinforced aluminum composite block is shown in Figure 1. Among these block specimens, a group of test blocks, shown in Figure 2a, was used to measure the temperature-time curve of the material during the quench and uphill quench processes. Specifically, it measured the temperature-versus-time curves for cold-water and PAG-solution quenching, and for heating low-temperature materials in boiling water at 100℃ and in hot oil at 170℃. The other test block group, shown in Figure 2b, was used for the various heat-treatment processes listed in Table 1.

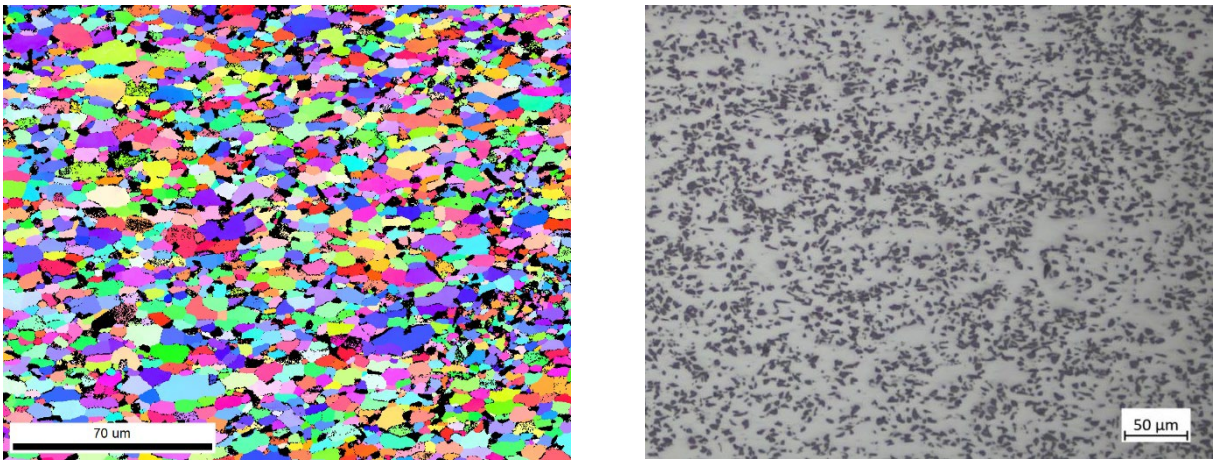

Fig. 1. The microstructure of 15%vol SiCp/Al-Cu-Mg composite forging via a) EBSD (The black particles represent SiC particles.); b) Optical microscopy.

Measuring the in-situ temperature of the material surface is challenging due to disturbances caused by flowing water. Therefore, this study chose to drill holes near the surface and core of the test block to place thermocouples. The positions of the K or PT100 armored thermocouples with a diameter of 3mm are shown in Figure 2a. To ensure data validity, the temperature-time curves for different quenching and heating conditions are repeatedly tested. The temperature changes during the quenching/reverse-quenching process are collected using a Novus data-sampling analyzer with a sampling frequency of 100Hz. The distribution of surface residual stress measurement paths for test blocks that have undergone different heat treatments is shown in Figure 2b. Each test block features 13 measurement points. Along each measurement path (AA’ or BB’) on the block surface, 7 points are spaced 10 mm apart. To ensure the reliability of the X-ray results, each point was measured three times.

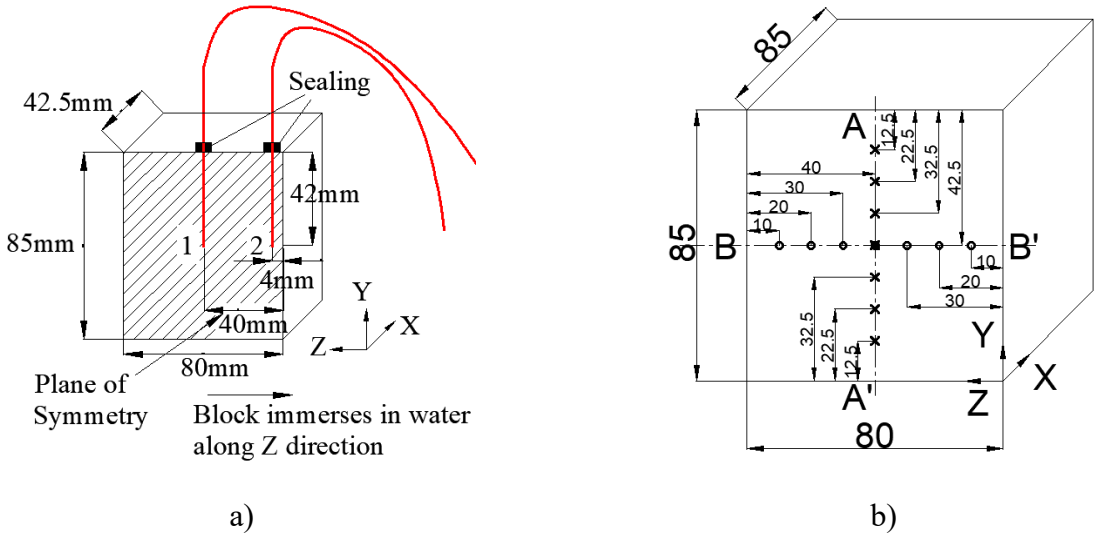

a) b)

Fig. 2. Pictorial showing a) The location of the temperature measurements for block; b) The X-ray diffraction measurement points for surface residual stresses of block.

The volume of boiling water in the high-temperature medium equipment exceeds 80 L, and the heating power is 4 kW + 20 kW (several temporary electric heating rods are installed on the bottom and side walls of the boiling water generator). The internal dimensions of the boiling water generator are Ø440 mm × 650 mm. For the mineral oil heating equipment, when the mineral oil is heated to 170℃, the volume of hot oil exceeds 80 L. The heating power and internal dimensions of this mineral oil heating equipment are the same as those of the boiling water generator. Since the boiling point of mineral oil is 260℃, no temporary electric heating rods are installed to control the oil temperature accurately.

The effectiveness of the uphill quenching process in regulating the residual stresses of the material caused by quenching hinges on a crucial factor: the rapid heating of the entire part from liquid nitrogen temperature to a high-temperature medium, from the outside to the inside. The UQ technique's data, particularly the maximum temperature difference between the inside and outside of the material, the duration of the 'sufficiently large' temperature difference (>40℃[7]), and the in-situ yield strength of materials during the UQ period, are of great importance. It is clear from Figure 3 that rapidly cooling from the solution heat-treatment temperature by immersing in cold water creates a steep thermal gradient between the surface and the core, leading to uneven plastic flow and residual stress. The maximum temperature difference between point 1 (Near surface) and point 2 (Core) was about 199°C, and this occurred 7s after immersion when point 2 was at 234.7°C and point 1 at 433.9°C.

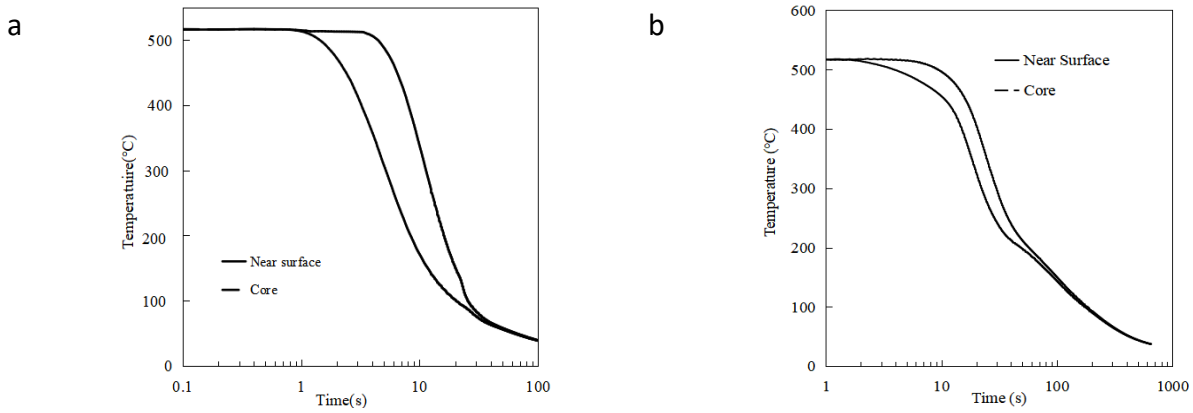

Fig. 3. Cooling curves from a quenched block at quenchant (～20°C). Cooling curves from a small surface (T2) and the core (T1) are shown. a) cold water quenched; b)30%PAG quenchant quenched.

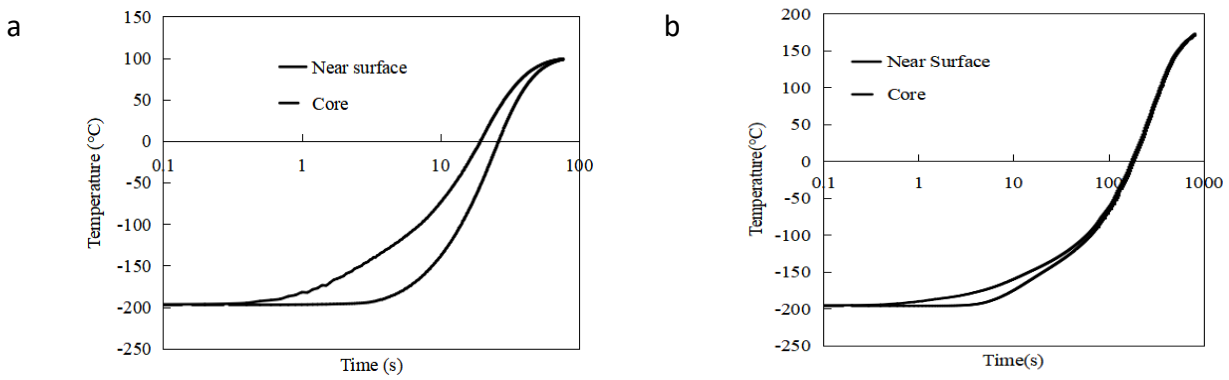

Fig. 4. Heating curves from the block during a uphill quench into high temperature medium with the same agitation condition. Cooling curves from a small surface (T2) and the core (T1) are shown a) Heating by boiling water; b) Heating by hot mineral oil.

When using a 30% PAG quenchant, the maximum temperature difference between the material's near-surface and core is only 80.5℃. This happens 19 seconds after the part enters the water. At this time, the point 2 near the material's surface temperature is 400.1℃, and the core temperature is 319.6℃.

For the block, which was processed by a reverse quench into boiling water, its interior reached 0°C after 25 seconds. The heating curves are shown in Figure 4. Point 2, close to the surface, was heated up quickly and reached 0°C after 19.1s. The maximum temperature difference between point 2 and point 1 was 67.5°C after 8.4s.

In the hot-oil case, point 2 heated up at a rate similar to that of the core. The maximum ΔT from point 2 to point 1 was 17.4°C when the temperature of point 2 was -173.0°C. The maximum temperature difference occurred at 5.4s after immersion in the hot oil.

The temperature results clearly demonstrate that although hot oil has a higher temperature, its heating efficiency for materials is still significantly lower than that of water. Furthermore, heating to high temperatures for more than 15 minutes is sufficient to cause a large number of solute atoms to precipitate from the supersaturated solid solution, thereby significantly increasing the in-situ yield strength of the as-quenched material and making it more difficult to release the quench-induced residual stress. Unlike boiling water heating and high-temperature & high-pressure steam heating, hot oil heating, similar to heating material via a furnace, does not strictly belong to the UQ technology. Therefore, this study deliberately chose not to use oil but instead used boiling water as the high-temperature liquid medium to control the residual quenching stress of aluminum matrix composites.

Table 1 presents five heat-treatment processes. Their effects on the microstructure and properties of particle-reinforced aluminum matrix composites, which are discussed in subsequent chapter. It should be noted that the low-temperature medium used in the UQ process described in Table 1 is liquid nitrogen, while the high-temperature medium is boiling water.

For the solution heat treatment (SHT) and quenching process, blocks were heated to 515℃ in an electrically heated, forced-convection furnace and held at that temperature for 4h to equilibrate. One group of blocks was quenched in agitated cold water (~20℃), and the other was quenched in a 30% PAG solution with the same agitation condition.

During the uphill quenching process, the quenched sample block is cooled to -196℃ at 3℃/min in an SLX-80 CNC cryogenic chamber and held at this temperature for a period of time (30min) until the overall temperature of the material reaches equilibrium. Then, it is quickly transferred to a high-temperature medium and held until the entire material reaches a nearly uniform temperature. Finally, it is taken from the high-temperature equipment. This is one uphill quenching treatment. In the process used in this study, two consecutive uphill quenching treatments were employed. After the first uphill quenching treatment, the heated sample block was placed in another CNC cryogenic chamber and cooled to -196℃ at 3℃/min, held for 30min to bring the material's overall temperature to -196℃, and then the heating process was repeated. When the entire material returns to the high-

temperature ambient, it is removed and air-cooled. The two consecutive UQ treatments are also referred to as the uphill quench cycle (UQC). According to the heat treatment processes 4 and 5 in Table 1, the test blocks that have undergone the uphill quenching cycle will be subjected to short-time (170℃ × 2 h) and long-time (170℃ × 12 h) aging.

Table 1. Heat treatments for the 15%vol SiCp/Al-Cu-Mg composite.

Block code	Heat treatment condition
1	SHT+CWQ +NA* 7 days
2	SHT+30%PAG (<20℃)+NA 7 days
3	SHT+CWQ+LN_2* (30 min)+BW*(85s) Cycle (UQ Cycle)+NA 7 days
4	SHT+CWQ+UQC+170℃/12h+NA 7 days
5	SHT+CWQ+UQC+170℃/2h+NA 7 days

* The cooling media LN_2: Liquid Nitrogen;
The high-temperature media BW: Boiling Water;
NA: Natural aging

Residual Stresses Measurement via X-Ray Diffraction Method

This study employed a portable Pulstec μ360 X-ray stress analyser equipped with an area detector and a novel Debye-ring fitting approach. Because X-rays penetrate only to a depth of several hundred microns, the X-ray diffractometer using the cosα technique measures only surface residual stresses.

The X-ray diffraction method determines surface stress maps for two stress components in specimens or components. Stress is characterized by analyzing Debye rings and the corresponding changes in ε_α detected in the diffraction data, as shown in Figure 5.

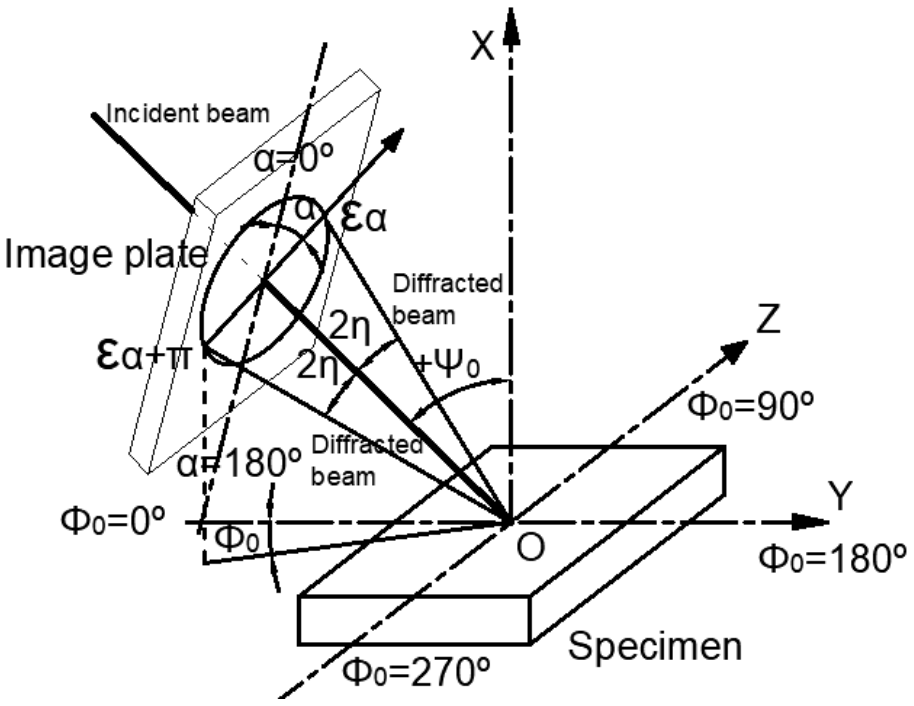

Fig. 5. Arrangement of the stress measurement via X-ray diffraction Method.

As noted by Toshiyuki et al.[8, 9], ε_α is a single-valued function of the angle α and can be described using a Fourier series:

$$\varepsilon_\alpha = a_0 + a_1 cos\alpha + b_1 sin\alpha + a_2 cos2\alpha + b_2 sin2\alpha + \cdots = a_0 + \sum_{k=1}^{\infty}(a_k coska\alpha + b_k sinka\alpha) \quad (1)$$

Plane stresses can be calculated via the measured ε_α, $\varepsilon_{-\alpha}$, $\varepsilon_{\pi+\alpha}$ and $\varepsilon_{\pi-\alpha}$, σ_z and σ_y can be described as:

$$\sigma_z = -\frac{E}{(1+v)}\frac{1}{sin2\eta}\frac{1}{sin2\psi_0}\frac{\varepsilon_{a1}(\alpha)}{cos\alpha} \quad (2)$$

$$\sigma_y = \frac{\sigma_x\left[\frac{1+v}{2E}sin^2\eta cos^2\psi_0 + \frac{\Psi}{2Ecos2\alpha}\right] - \frac{\varepsilon_{a2}(\alpha)}{2cos2\alpha}}{\frac{1+v}{2E}sin^2\eta + \frac{1}{4Ecos2\alpha}\{(1-cos2\eta) - v(3+cos2\eta)\}} \quad (3)$$

where Ψ is determined as blelow;

$$\Psi = 2cos^2\eta sin^2\psi_0 + sin^2\eta cos^2\psi_0 - v\{2cos^2\eta cos^2\psi_0 + sin^2\eta(1+sin^2\psi_0)\} \quad (4)$$

Here, E represents the bulk Young's modulus, v denotes Poisson's ratio, 2η is the angle between the incident and diffraction beams, ψ_0 is the angle between the sample normal and the incident beam and Φ_0 is the angle between the projection of the incident beam on the sample surface and the x-axis, as shown in Figure 5[10].

The Material Properties and Microstructure Characterization

To avoid machining-induced residual stress, the test blocks treated with the heat treatments listed in Table 1 were subjected to mechanical and microstructural characterization after residual stress measurement. Tensile testing was performed in accordance with GBT/228.1 Standard using a test piece with a nominal diameter of 5 mm, a cross-sectional area of ~20 mm^2, and a gauge length of 25 mm. All specimens were tested at a strain rate of 1×10^{-2} S^{-1}. Fracture toughness testing was conducted in accordance with GB/T 4161 Standard. These had either an X-Y or a Y-X orientation relative to the forging's longitudinal axis. The sampling locations of the above specimens are shown in Figure 6. The tensile properties and fracture toughness K_{IC} values obtained from specimens treated with different heat treatment processes are averaged and listed in Table 2.

To analyze the precipitation behavior of the material during natural/artificial aging at the microscopic level, a combination of transmission electron microscopy (TEM) was used. Among them, transmission electron microscopy (TEM) was performed on a JEM-2100F microscope at 200 kV. The TEM samples were cut from blocks subjected to different heat treatments and ground into thin foils 0.7-0.8 mm thick. Several disks with a diameter of 3 mm were punched from these thin foils and then electropolished in a solution of hydrogen nitrate and methanol (volume ratio 1:4) to observe and characterize the precipitates within the sample.

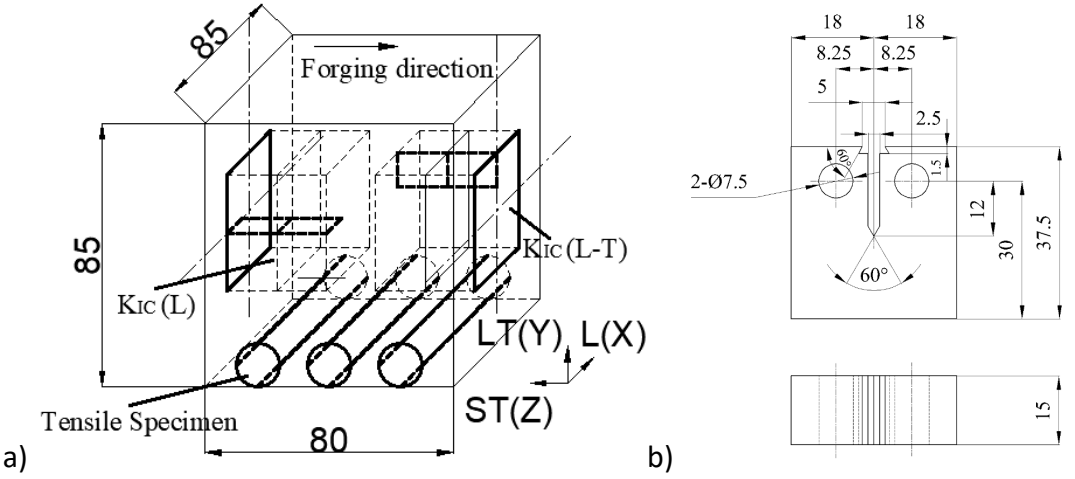

Fig. 6. a) Fracture plane identification and samples' location; b) The size of fracture toughness Specimen for K_{IC} measurement (Dimension: mm).

Results and Discussion

Residual stresses

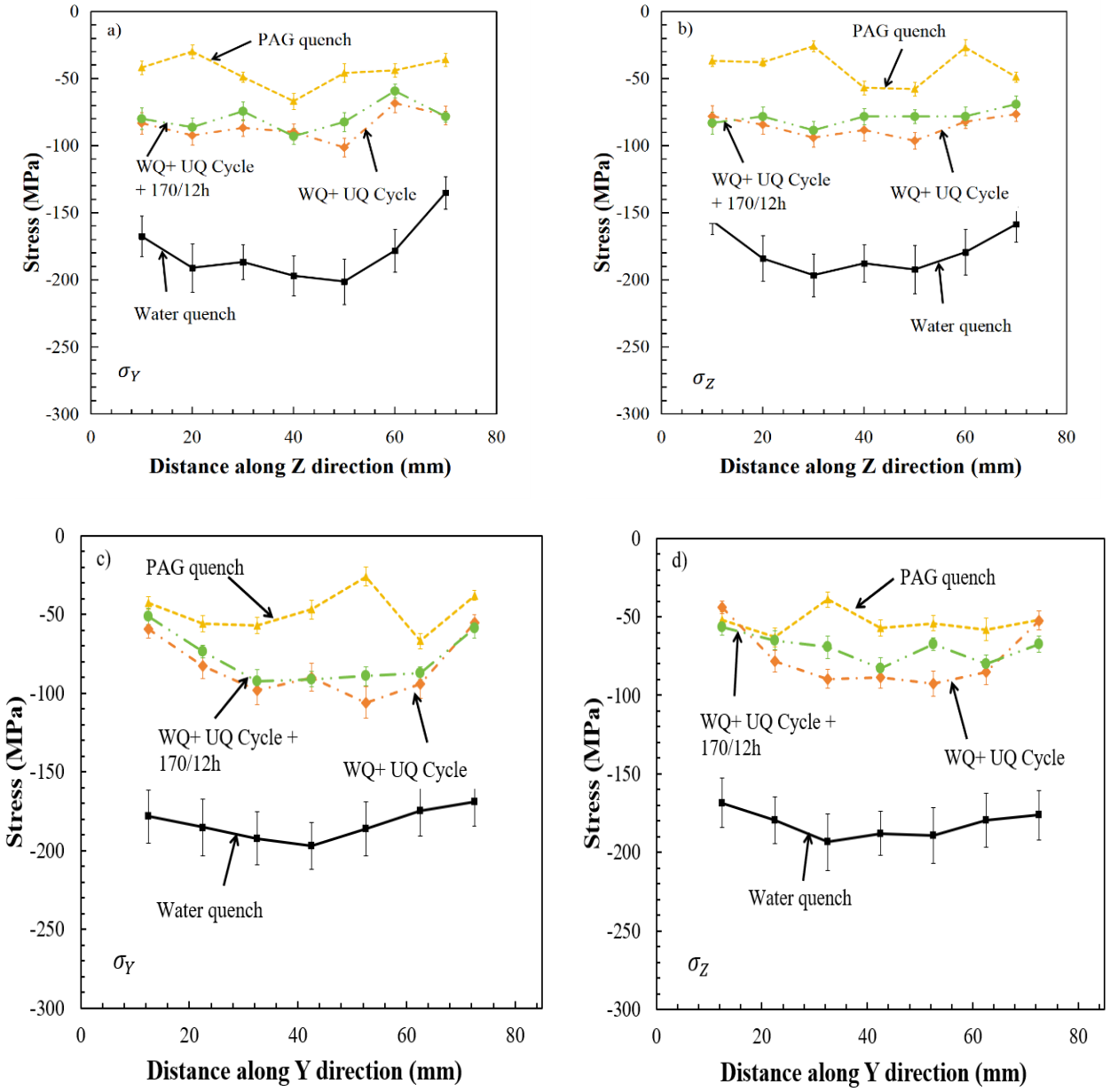

Fig. 7. Surface residual stresses of different direction of the block. a) BB' σ_Y, b) BB' σ_Z, c) AA' σ_Y, d) AA' σ_Z.

Figure 7 displays the surface residual stresses of the block quenched in a 30% PAG solution. Quenching in PAG significantly alters the magnitudes of residual stress compared to CWQ. After UQC, a moderate decrease in residual stresses was observed along the AA' and BB' paths, indicating that UQC is also effective for relieving quench-induced stresses. XRD analysis further revealed that the maximum compressive residual stress from water quenching was reduced by about 50% with just a UQC, and by up to 59% when UQC was combined with artificial ageing. Although UQC can substantially reduce the residual stress generated during CWQ, PAG quenching is even more effective for controlling residual stress in the material.

Mechanical Properties and Microstructure

To analyze the influence of different heat treatments on the mechanical properties of particle-reinforced aluminum composites, the materials' strength, plasticity, and fracture toughness were evaluated.

Table 2 shows that the cold water-quenched material exhibits better strength and ductility than that quenched by a 30%PAG solution. This suggests that a high cooling rate can enhance the material's precipitation performance during NA. Furthermore, the mechanical properties between the SHT+CWQ+NA state and the SHT+CWQ+UQC+NA state show almost no difference after a period of natural aging (7 days), indicating a limited uphill quench effect on solute precipitation during the following NA stage. For artificially aged aluminum composites, natural aging has no further effect on their mechanical properties.

Table 2. Average tensile properties and fracture toughness KIC results.

Block number	Heat treatment Condition	Yield stress Rp0.2 (MPa)	Ultimate Tensile strength Rm (MPa)	Elongation δ%	Area Reduction Z%	KIC L (MPa ▪ $m^{1/2}$)	KIC L-T (MPa ▪ $m^{1/2}$)
1	SHT+CWQ+NA* 7days	351	535	8.2	9.8	16.4	16.3
2	SHT+quench(30%PAG) +NA 7days	307	478	6.5	9.5	15.3	14.9
3	SHT+CWQ+UQC+NA 7days	349	522	8.4	10.5	18.7	17.8
4	SHT+CWQ+UQC+170℃/ 12h+NA 7days	405	540	7.1	9.0	15.7	15.8
5	SHT+CWQ+UQC+170℃/ 2h+NA 7days	377	535	7.9	8.2	19.2	19.7

It is generally believed that the fracture toughness of aluminum alloys depends on yield strength, Young's modulus, precipitation size, and volume fraction in the microstructure[11]. There is also a view that the fracture toughness of aluminum alloys is roughly positively correlated with the product of the material's strength and plane-strain ductility [12]. For silicon carbide particle-reinforced aluminum composites, the fracture toughness measurement depends not only on the ductility of the material and the yield strength, but also on the uniformity of the reinforcement distribution[13].

As shown in Figure 1, the distribution of silicon carbide reinforcement phase particles is essentially uniform. As shown in Table 2, the cooling rate affects the material's strength and tensile ductility, thereby influencing changes in fracture toughness. When the aging condition is 170℃/2h, the material's strength improves relative to the SHT+CWQ+NA state. However, the elongation of the material shows little change, so the highest fracture toughness is obtained under the heat-treatment condition, similar to the result for aluminum alloys [11].

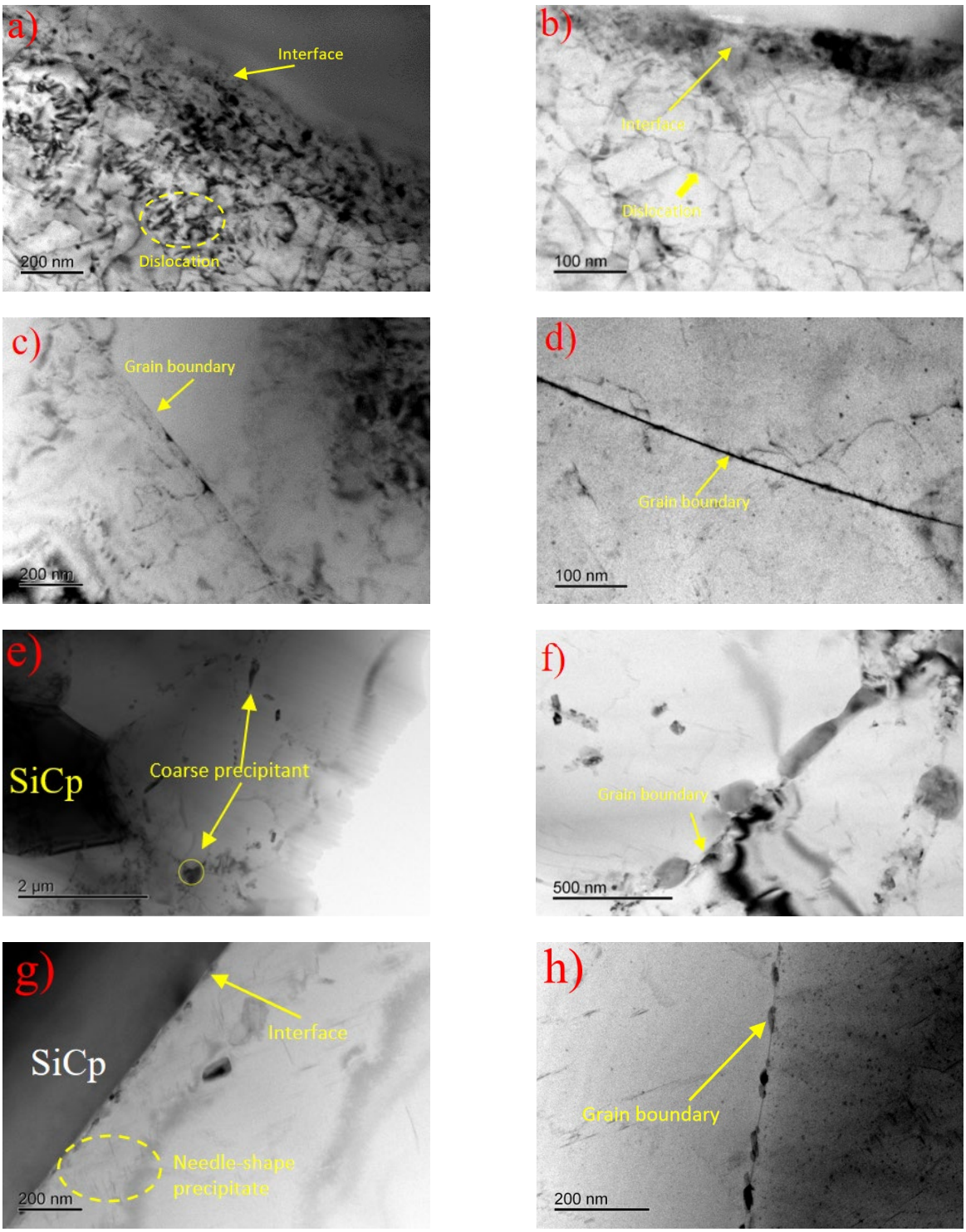

Fig. 8. Bright field TEM and HRTEM images (the inserted corresponding SAED and FFT patterns) taken from particle-reinforced aluminum composites under different heat treatment conditions: (a)&(c) SHT+CWQ samples, (b)&(d) SHT+CWQ+UQC samples, (e-f) SHT+PAG quench samples, (g-h) SHT+CWQ+UQC+170°C /12h.

Figure 8 (a) & (c) are bright field transmission electron microscopy (TEM) images of SHT+CWQ samples after natural aging. In the bright-field image, a high density of dislocation entanglements is observed near the interface between the reinforcement phase and the matrix. The generation of these dislocations is related to the thermal stress induced by the mismatch in the thermal expansion coefficient (CTE) between the matrix and the reinforcement phase during quenching of the aluminum matrix composite. Figure 8(b) & (d) are bright-field TEM images of the UQC after solution quenching. Figure 8(b) shows some polygonal rings that can be observed between the interface of the

reinforcement phase and the matrix in this heat treatment state. This dislocation structure is similar to the initial precipitates of the incoherent phase, which "capture" the dislocations. Therefore, it is reasonable to assume that the formation of this metastable phase has begun after the UQC. However, they cannot be clearly distinguished due to the large number of defects and their small size. Compared with the SHT+CWQ+NA state, Figure 8(d), the aluminum-based composite's grain boundary precipitation phases (GBPs) after the UQC become slightly coarsened and continuous. Figure 8(e-f) is a bright-field TEM image of the sample after PAG quenching. It shows that coarse quench-induced phases can be observed at the matrix/reinforcement interface and near grain boundaries (Figure 8 (e) & (f)). Under high magnification observation, the precipitated phase at the grain boundary of the SHT+PAG quenched sample is coarse and discontinuous. Figure 8 (g-h) is a bright field TEM image of the sample after UQC treatment and 170℃/12h aging treatment. It can be seen that after aging treatment at 170℃/12h, precipitated phases can be generated in the aluminum matrix, at the interface, and at grain boundaries of the SHT+CWQ+UQC+170°C/12h sample. Comparing the TEM microstructures of aluminum-based composite samples under different heat treatment states, it can be summarized as follows: (a) PAG quench will cause a considerable amount of coarse quenching equilibrium phase to precipitate in the aluminum-based composite matrix; (b) Long-term aging treatment will coarsen the precipitate phase in the organization to a certain extent, but it is still in the range of ~80nm. Compared with the SHT+CWQ+NA state, the precipitate phase at the grain boundary becomes larger and more dispersed; (c) Uphill quench cycle treatment has no obvious effect on the organization of aluminum-based composites.

Summary

In this study, a series of experiments was conducted to investigate the effects of uphill quenching on the characteristics of particle-reinforced aluminum composites, including residual stress, mechanical properties, and microstructure. The following conclusions were drawn:

1. The maximum heat exchange rate between the material and the medium during uphill quench in this study was obtained. The core of the material reached 0℃ after 25s of entering the boiling water. The maximum temperature difference between the surface and the core was 67.5℃, and the temperature near the surface was -154℃ at this time. During the heating stage of the uphill quenching process, the temperature difference between the surface and the core of the material is at least 40℃, lasting for about 26.5s.

2. Although the 30% PAG quenching liquid has a significant effect on the regulation of the residual stress in aluminum composites, it also harms the materials' strength, plasticity, and fracture toughness;

3. The uphill quenching process can relax the residual stress in aluminum composites while preserving its supersaturated solid solution structure to a great extent, which makes its combination with short-time aging effective in improving the strength, plasticity, and fracture toughness of the material compared to the SHT+CWQ+NA condition.

Acknowledgment

Grant acknowledgments to National Key Research and Development Program 2022YFB3405101.

References

[1] T. Dursun, C. Soutis, Recent developments in advanced aircraft aluminium alloys, Mater. Des. 56 (2014) 862-871.

[2] E. Alexander, S. Christopher, M.J.N.w.K.A.P. Andreas, Metal matrix composites in industry: an introduction and a survey, Springer New York, New York, 2003.

[3] D.A. Lados, D. Apelian, L. Wang, Minimization of residual stress in heat-treated Al–Si–Mg cast alloys using uphill quenching: Mechanisms and effects on static and dynamic properties, Mater. Sci. Eng. A 527 (2010) 3159-3165.

[4] D.A. Lados, D. Apelian, The effect of residual stress on the fatigue crack growth behavior of Al-Si-Mg cast alloys-Mechanisms and corrective mathematical models, Metall. Mater. Trans. A 37 (2006) 133-145.

[5] J.S. Robinson, A. O'Donovan, R.C. Wimpory, Uphill Quenching to Reduce Residual Stress in Aluminium Alloy 7449 Hollow Structures, Exp. Mech. 62 (2022) 1411-1420.

[6] M.X. Dung, Y.A. Puchkov, S.L. Berezina, Influence of uphill quenching on residual stresses and properties of alloy D16, Mater. Today: Proc. 38 (2020) 1294-1298.

[7] W.S. Mattos, G.E. Totten, L.C.F. Canale, Uphill quenching of Aluminum alloys, Matls. Perf. Charact. 6 (2017) 894-903.

[8] T. Miyazaki, Y. Maruyama, Y. Fujimoto, T. Sasaki, Improvement of X-ray stress measurement from a Debye–Scherrer ring by oscillation of the X-ray incident angle, Powder Diffr. 30 (2015) 250-255.

[9] T. Miyazaki, T. Sasaki, X-ray stress measurement with two-dimensional detector based on Fourier analysis, Int. J. Mater. Res. 105 (2014) 922-927.

[10] T. Sasaki, Y. Hirose, K. Sasaki, S.Y. Wa, Influence of image processing conditions of debye Scherrer ring images in x-ray stress measurement using an imaging plate, Adv. X-ray Anal. 40 (1997) 588-594.

[11] G.T. Hahn, A.R. Rosenfield, Metallurgical factors affecting fracture toughness of aluminum alloys, Metall. Trans. A 6 (1975) 653-668.

[12] D.J. Lloyd, Particle reinforced aluminium and magnesium matrix composites, Int. Mater. Rev. 39 (1994) 1-23.